Potential Energy Surface for the Chlorine Atom Reaction with Ethylene: A Theoretical Study

P. Braña, B. Menéndez, T. Fernández, and J. A. Sordo*

Laboratorio de Química Computacional, Departamento de Química Física y Analítica, Facultad de Química, Universidad de Oviedo, Julián Clavería 8, 33006 Oviedo, Principado de Asturias, Spain

The potential energy surface of the reaction between chlorine atom and ethylene was explored at the MP2/6-31G(d,p), Becke3LYP/6-31G(d,p), QCISD/6-31G(d,p), MP2/6-311+G(d,p), MP2/6-311++G(3df,3pd), and MP2/aug-cc-pVDZ levels of theory. Further QCISD(T)/6-31G(d,p) and QCISD(T)/cc-pVDZ optimizations were performed for some structures of special interest. The geometrical parameters computed for the different structures located on the potential energy surface do not differ too much when employing different methods and basis sets with the only exceptions of those structures involving long distance interactions (van der Waals structures). The pronounced flatness of the potential energy surface in the regions where these structures appear seems to be the responsible for the observed discrepancies. The full optimized QCISD structures tend to become less stable than those computed at the MP2 level, whereas the opposite is true for the Becke3LYP structures. At the MP2 and QCISD levels, the transition structure associated with a direct shuttle motion in the addition channel is too high in energy to be involved in the dissociation mechanism. The existence of two bridged structures **Iadd** (minimum) and **TSadd** (transition structure) on the potential energy surface helps to explain the experimentally detected stereochemical control exercised by the chlorine atom in reactions involving haloethyl radicals. Contrarily, the Becke3LYP calculations suggest a mechanism in which the direct shuttle motion could play a relevant role, although the competing mechanism of rotation around the C–C bond is lower in energy. The MP2 and QCISD abstraction channels also differ considerably from the Becke3LYP one. However, in this case all the different potential energy surfaces seem to be consistent with the reported experimental data on the activation energy and endothermicity for the abstraction reaction. The QCISD(T)/aug-cc-pVDZ//QCISD/6-31G(d,p) relative energies and barrier heights are consistent with the experimental data available on exo/endothermicities and activation barriers for the addition and abstraction reactions.

Introduction

The reactions between halogen atoms and hydrocarbons are of considerable importance because they take part in a number of processes of practical interest. Thus, it is well-known that thermal and hot reactions between halogen atoms and olefinic molecules play a relevant role in recoil chemistry since these species are frequently utilized as scavengers.[1] The processes involved in the incineration of hazardous halogenated wastes[2] or in the combustion of chlorine-containing fuel contaminants[3] and the reactions of chlorine atoms with methane intervening in the cycle of stratospheric ozone layer destruction[4] are also good examples. Also, these reactions represent loss processes for chlorine atoms and nonmethane hydrocarbons in the atmosphere,[5–7] thus causing changes in the atmospheric composition that can alter the stability of the environment. Particularly, the reaction between chlorine and ethylene proceeds through two competitive channels:

$$Cl + C_2H_4 \rightarrow C_2H_3\bullet + HCl \qquad (1)$$

$$Cl + C_2H_4 \, (+M) \rightarrow C_2H_4Cl\bullet \, (+M) \qquad (2)$$

While the abstraction reaction (eq 1) is an endothermic process (5–6 kcal/mol)[1,8] with an estimated activation energy of 3–7 kcal/mol,[9–12] the chlorine addition to ethylene (eq 2) occurs readily having little or no activation barrier and an exothermicity

of 22 kcal/mol.[1] Therefore, at lower temperatures (say below 500 K) the reaction is dominated by addition (eq 2) to form a chloroethyl radical, and at higher temperatures the addition reaction is less important and the abstraction reaction can be experimentally studied directly.[12] On the other hand, only at sufficiently low total pressure can the abstraction channel be observed.[11]

It has also been stressed that in chlorine atom reactions with unsaturated hydrocarbons, HCl production can also occur via an addition–elimination mechanism[13f] but the activation energy

$$Cl + C_2H_4 \rightarrow C_2H_4Cl^* \rightarrow HCl + C_2H_3\bullet \qquad (3)$$
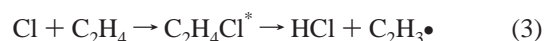
estimated for the elimination process is too high (∼50 kcal/mol).[1] Other secondary reactions may play a relevant role in the kinetics of these reactions at different experimental conditions.[11] Particularly, the possible formation of two different radicals: 1-chloroethyl radical $CH_3ClCH\bullet$ and 2-chloroethyl radical $CH_2ClCH_2\bullet$, should also be considered.[12]

From a theoretical viewpoint, a number of recent works have shown that ab initio methodologies as applied at a high level (nowadays affordable as a consequence of the remarkable performance of the more and more powerful workstations, clusters, and supercomputers, within the sixth generation of computers)[14] do provide quite useful information on the addition and abstraction reactions between radicals and organic com-

Potential Energy Surface for Chlorine Atom

J. Phys. Chem. A, Vol. 104, No. 46, 2000 **10843**

pounds, thus nicely complementing the experimental data available.[13] An especially important contribution from these theoretical works is the location and characterization of intermediate complexes on the potential energy surface (PES) as they can be responsible for the negative activation energies derived from the kinetic experimental studies.[15] Mozurkewich and Benson[16] used the Rice–Ramsperger–Kassel–Marcus (RRKM) theory[17] to develop quantitative expressions for the rates of reactions that have negative activation energies for the cases corresponding to a reaction profile presenting a minimum associated with the formation of a stable intermediate complex between two transition states, the first one loose and the second one tight (the tight transition state should have a significant threshold energy with respect to the intermediate but may have a negative potential energy relative to reactants). Rayez and co-workers[13g] recently extended the RRKM treatment to deal with bimolecular reactions in which two intermediate complexes are formed. The location of these weakly bound complexes on the PES has also an intrinsic theoretical interest: as stressed elsewhere,[18] it is strictly needed to avoid serious topological inconsistencies in the computed PES. Indeed, in the work by Schlegel and Sosa[19] on the reaction between chlorine atom and ethylene, these authors reported a transition structure located at the HF/6-31G(d) level for the addition reaction 2, which is lower in energy than reactants. Such a situation is only possible if an intermediate complex between the reactants and the transition structure exists; this transition structure does not connect reactants and products but the intermediate complex with products. This latter point is sometimes rather difficult to show since the intrinsic reaction coordinate (IRC) technique[20] usually does not work properly when weakly bound systems are involved (partly due to numerical problems associated with that weakness).[21]

Several ab initio theoretical studies have been carried out on the reaction between ethylene and chlorine atom. As mentioned above, Schlegel and Sosa[19] located a chlorine addition transition structure at the UHF level and concluded that the 2-chloroethyl radical adopts an antiperiplanar conformation with a rotation barrier of 4 kcal/mol. Hoz et al.[22] located two symmetrically bridged (C_{2v}) structures [the first one ($^2B_2$) about 13 kcal/mol above the dissociation limit and the second one ($^2A_1$) less than 1 kcal/mol more stable than the dissociation products] and one unsymmetrically bridged (C_1) structure (about 1 kcal/mol more stable than the dissociation products) at the UHF level. When these authors computed the energy profiles corresponding to the $^2B_2$ and $^2A_1$ states at the configuration interaction (CI) level using a multiconfigurational (MCSCF) wave function, only a very shallow minimum at a large C–Cl distance was located. Furthermore, it disappears when a planar structure for C_2H_4 is forced. Such a loose association of a chlorine atom and an ethylene molecule might be either a transition structure or a molecule–radical π-complex intermediate in an elimination–readdition mechanism for the 1,2-shift.[22] One of the most complete studies for the present was carried out at the multi-reference single- and double-excitation (MRD-CI) level by Engels et al.[23] Two dissociation pathways leading to CH$_2$ClCH$_2$• were explored: the direct path involving an unsymmetrical intermediate and a two-step path involving a local symmetric minimum (which is at the same time, according to these authors, the transition state for the 1,2 migration), followed by the pathway to the absolute asymmetric minimum (2-chloroethyl radical), which is part of the shuttling motion[24] leading to Cl + C$_2$H$_4$. The activation energy for rotation about the C–C axis is calculated to be around 4.3 kcal/mol, comparable to that for

the 1,2-migration (around 6 kcal/mol). On the basis of MP2 calculations, Guerra[25] concluded that, although the shuttle motion is likely in 2-chloroethyl radical (the symmetrically bridged $^2A_1$ structure is 7.3 kcal/mol below the dissociation limit and 13.3 kcal/mol higher than the anti structure of the CH$_2$-ClCH$_2$• radical), the experimentally observed stereochemical control of small entity exercised by the chlorine atom could be due to the high population of the eclipsed rotamer of the CH$_2$-ClCH$_2$• radical in conjunction with the nonplanarity of the radical site and/or steric hindrance of the β-substituent[26] rather than due to shuttling.[24] More recently, Knyazev et al.[27] studied the kinetics of the unimolecular decomposition of the CH$_2$-ClCH$_2$• radical. Their PMP4/6-31G(d,p)//UMP2/6-31G(d,p) calculations indicate that there is no transition structure on the two possible pathways (symmetric and unsymmetric). Calculations of Ihee et al.[28] [local MP2 and DFT using the LAV3P relativistic effective core potential[29] for describing the chlorine atom and the 6-31G(d,p) basis set for hydrogen and carbon atoms] seem to confirm the Skell hypothesis of symmetric bridging[24] (they locate a symmetrically bridged structure 10.5 kcal/mol below the dissociation limit at the Becke3LYP level of theory) to explain the stereochemical control of haloethyl radicals, concluding that bridged structures play an important role in the dissociation processes involving the CH$_2$ClCH$_2$• radical.

In this paper, we report the results of an extensive exploration of the PES for the reaction between chlorine atom and ethylene carried out at different theoretical levels. Our objective is two-fold: (a) to obtain theoretical data accurate enough to be useful to tackle further kinetic and thermodynamic theoretical studies to complement the existing information on the temperature and pressure dependence of these reactions and (b) to analyze the advantages and drawbacks of some of the most popular theoretical methods (with different basis sets) available to plan further computational studies on systems that because of their complexity (size) can only be studied at a given (not too sophisticated) level of theory.

Theoretical Methods

The PES for the reaction between chlorine atom and ethylene was explored at different theoretical levels including several methods: Møller–Plesset perturbation theory (MP2, MP4),[30] quadratic configuration interaction (QCI),[31] and density functional theory (DFT),[32] as well as different basis sets: Pople's[33] 6-31G(d,p), 6-311+G(d,p), 6-311++G(3df,3pd), and Dunning's[34] aug-cc-pVDZ. All the geometry optimizations were carried out at the MP2/6-31G(d,p), Becke3LYP/6-31G(d,p), QCISD/6-31G(d,p), MP2/6-311+G(d,p), MP2/6-311++G(3df,-3pd), and MP2/aug-cc-pVDZ levels of theory, thus allowing us to analyze the performance of the different methodologies and basis sets for computing PESs of this type of reaction involving radicals. QCISD(T)/6-31G(d,p) and QCISD(T)/cc-pVDZ optimizations were also undertaken in some specific cases (see next section). In the case of the larger basis sets [6-311+G-(d,p), 6-311++G(3df,3pd), and aug-cc-pVDZ], single-point calculations at the MP4SDTQ, Becke3LYP, and QCISD(T) levels were performed as well. The reliability of these single-point calculations were assessed by employing the 6-31G(d,p) basis set, for which geometry optimizations at the higher levels of theory were affordable.

All the structures located on the PES were characterized at the MP2/6-31G(d,p) and MP2/6-311+G(d,p) levels of theory by computing the corresponding Hessian matrix, examining the number of imaginary frequencies from it.
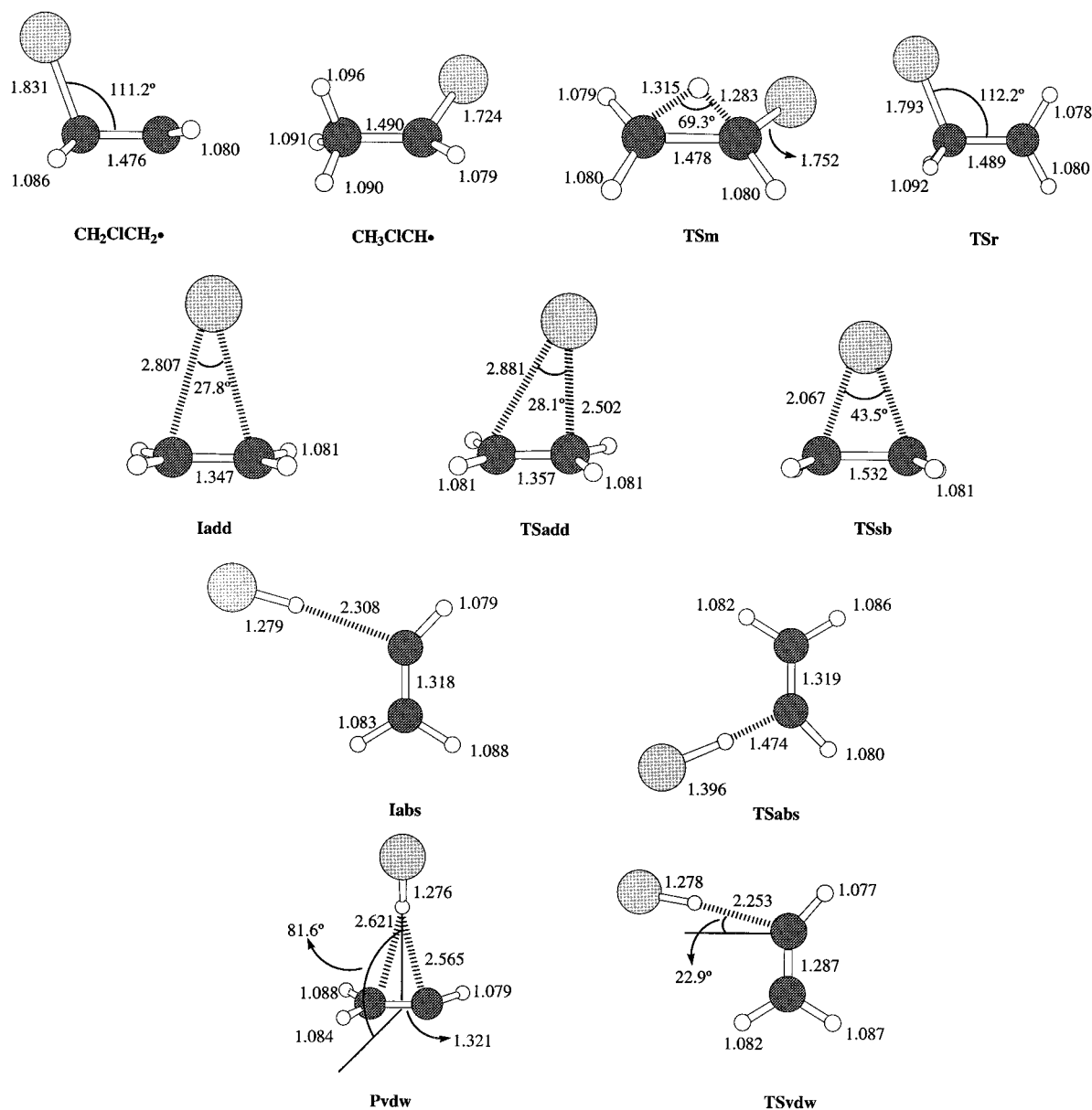
Figure 1. QCISD/6-31G(d,p) geometrical parameters for all the structures located in this work (see Table 1 and Figures S1−S11 of Supporting Information for the geometrical parameters as computed at other levels of theory). Bond distances are given in angstroms, and angles are given in degrees.

It is well-established that the use of spin annihilation techniques to generate spin projected energies is mandatory for calculations on both reaction energies and barrier heights.[13e] Unless otherwise stated, all the energy values reported in this work correspond to spin projected calculations.

Basis set superposition errors (BSSE) were not taken into account in the present work by two reasons: (a) In agreement with a number of previous papers on quite different systems,[35] recent works on the reactivity of radical addition to alkenes conclude that the values of BSSE [as estimated by the counterpoise procedure (CP)][36] do not converge within the size of basis sets employed and, what is still worse, the corrections of the barrier height values for the calculated BSSE drastically deteriorates the agreement with experiment.[13e,h] These anomalies must be ascribed in part to the overcorrection of the CP method when applied at correlated levels due to excitations to physically artifactual excited states involving ghost orbitals.[37,38] (b) The BSSE does not affect the calculation of barrier heights in the case of processes involving intermediate complexes[39] like the

ones studied in the present work. In any case, since the intermediates located in the present work are quite strongly bound (see below), it is not expected that the BSSE correction would convert them into unstable structures.

All the calculations were carried out using the GAUSSIAN94[40] and GAUSSIAN98[41] packages of programs.

Results and Discussion

For the sake of simplicity, only the structures optimized at the QCISD/6-31G(d,p) level are presented in Figure 1: it includes the structures for the addition channel (products, **TSm**, **Iadd**, **TSadd**), a symmetrically bridged structure (**TSsb**), the transition structure (**TSr**) for the rotation around the C−C bond of the 2-chloroethyl radical, and the structures involved in the abstraction channel (products, **Iabs**, **TSabs**, **Pvdw**, **TSvdw**). Table 1 collects the most representative geometrical parameters for these structures as computed at the different levels of theory employed in this work, and Figures S1−S11 of Supporting

Potential Energy Surface for Chlorine Atom

J. Phys. Chem. A, Vol. 104, No. 46, 2000 **10845**

TABLE 1: Most Significant Geometrical Parameters as Computed at the Different Levels of Theory Employed in This Work[b]

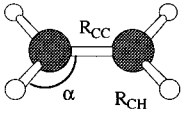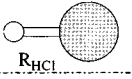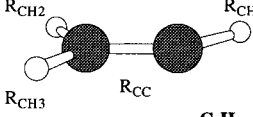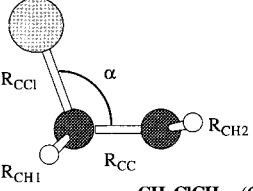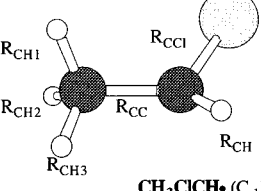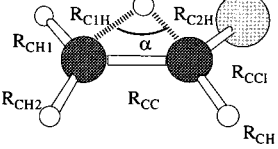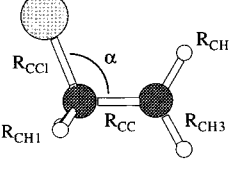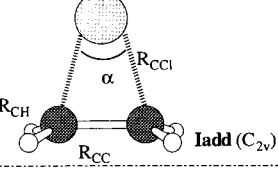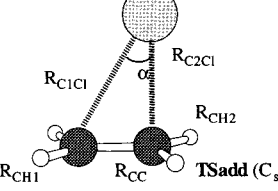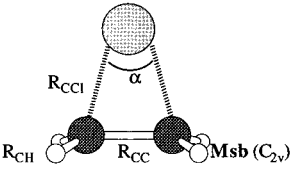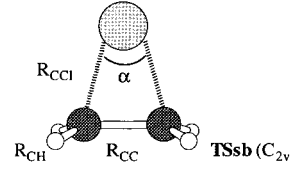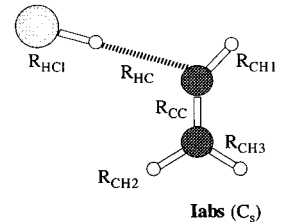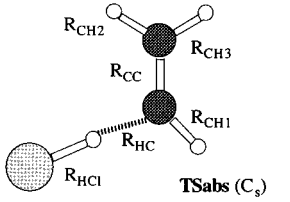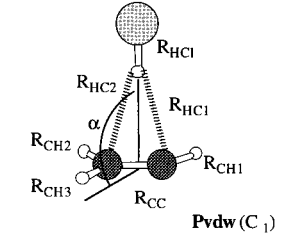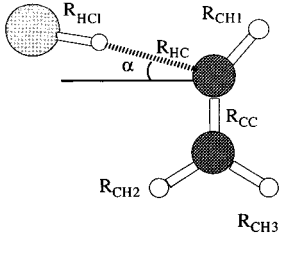| SYSTEM	PARAMETERS	MP2				Becke3LYP	QCISD[a]
		6-31G(d,p)	6-311+G(d,p)	6-311++G(3df,3pd)	aug-cc-pVDZ	6-31G(d,p)	6-31G(d,p)
C_2H_4 (D$_{2h}$)	R_{CC}	1.335	1.339	1.332	1.349	1.330	1.337
	R_{CH}	1.081	1.085	1.081	1.093	1.087	1.082
	α	121.6	121.4	121.3	121.3	121.8	121.7
HCl (C$_{\infty v}$)	R_{HCl}	1.269	1.273	1.272	1.288	1.287	1.272
$C_2H_3\bullet$ (C$_s$)	R_{CC}	1.288	1.289	1.281	1.299	1.310	1.319
	R_{CH1}	1.077	1.081	1.076	1.090	1.083	1.079
	R_{CH2}	1.086	1.091	1.087	1.099	1.095	1.088
	R_{CH3}	1.082	1.086	1.082	1.094	1.090	1.084
$CH_2ClCH_2\bullet$ (C$_s$)	R_{CCl}	1.817	1.816	1.813	1.845	1.892	1.831
	R_{CC}	1.474	1.477	1.470	1.479	1.460	1.476
	R_{CH1}	1.086	1.089	1.084	1.097	1.089	1.086
	R_{CH2}	1.078	1.082	1.077	1.090	1.084	1.080
	α	111.4	110.9	110.4	110.1	110.5	111.2
$CH_3ClCH\bullet$ (C$_1$)	R_{CCl}	1.718	1.716	1.704	1.736	1.736	1.724
	R_{CC}	1.485	1.488	1.481	1.492	1.485	1.490
	R_{CH1}	1.094	1.099	1.094	1.106	1.102	1.096
	R_{CH2}	1.089	1.093	1.099	1.101	1.096	1.091
	R_{CH3}	1.089	1.093	1.088	1.101	1.095	1.090
	R_{CH}	1.078	1.082	1.077	1.091	1.083	1.079
TSm (C$_1$)	R_{CCl}	1.746	1.741	1.729	1.762	1.781	1.752
	R_{CC}	1.472	1.475	1.469	1.479	1.471	1.478
	R_{CH1}	1.077	1.081	1.077	1.089	1.083	1.079
	R_{CH2}	1.079	1.083	1.078	1.091	1.086	1.080
	R_{CH}	1.080	1.083	1.078	1.091	1.085	1.080
	R_{C1H}	1.300	1.306	1.301	1.315	1.326	1.315
	R_{C2H}	1.266	1.279	1.272	1.286	1.287	1.283
	α	70	69.6	69.6	69.3	68.5	69.3
TSr (C$_s$)	R_{CCl}	1.785	1.783	1.778	1.805	1.817	1.778
	R_{CC}	1.485	1.488	1.481	1.492	1.482	1.489
	R_{CH1}	1.091	1.095	1.090	1.102	1.097	1.092
	R_{CH2}	1.075	1.080	1.075	1.088	1.082	1.078
	R_{CH3}	1.078	1.083	1.078	1.091	1.085	1.080
	α	112.3	112.2	112.2	111.8	112.6	112.2
Iadd (C$_{2v}$)	R_{CCl}	2.683	2.634	2.531	2.566	2.807 (2.745) [2.761]	
	R_{CC}	1.351	1.355	1.355	1.372	1.347 (1.354) [1.363]	
	R_{CH}	1.080	1.084	1.079	1.092	1.081 (1.082) [1.098]	
	α	29.2	29.8	31.1	31.0	27.8 (28.5) [28.6]	
TSadd (C$_s$)	R_{C1Cl}	2.738	2.680	2.607	2.638	2.881 (2.847) [2.841]	
	R_{C2Cl}	2.383	2.359	2.324	2.350	2.502 (2.498) [2.496]	
	R_{CC}	1.345	1.350	1.355	1.362	1.357 (1.360) [1.370]	
	R_{CH1}	1.079	1.083	1.078	1.091	1.081 (1.082) [1.097]	
	R_{CH2}	1.079	1.083	1.079	1.091	1.081 (1.082) [1.097]	
	α	29.4	30.2	31.0	31.0	28.1 (28.5) [28.8]	

TABLE 1: (Continued)

SYSTEM	PARAMETERS	MP2				Becke3LYP	QCISD[a]
Msb (C$_{2v}$)	R_{CCl}	1.952	1.918	1.978		2.074	2.067
	R_{CC}	1.525	1.519	1.535		1.538	1.532
	R_{CH}	1.083	1.079	1.091		1.084	1.081
	α	46.0	46.6	45.7		43.5	43.5
TSsb (C$_{2v}$)	R_{CCl}	1.958				2.653	
	R_{CC}	1.522				1.356	
	R_{CH}	1.080				1.084	
	α	45.7				29.6	
Iabs (C$_s$)	R_{HCl}	1.279		1.286		1.301	1.279
	R_{HC}	2.232		2.110		2.125	2.308
	R_{CC}	1.283		1.279		1.296	1.318
	R_{CH1}	1.077		1.070		1.089	1.079
	R_{CH2}	1.082		1.083		1.094	1.083
	R_{CH3}	1.086		1.087		1.099	1.088
TSabs (C$_s$)	R_{HCl}	1.382	1.392	1.393		1.398	1.396
	R_{HC}	1.489	1.470	1.462		1.495	1.474
	R_{CC}	1.284	1.285	1.278		1.294	1.319
	R_{CH1}	1.079	1.083	1.078		1.091	1.080
	R_{CH2}	1.081	1.086	1.082		1.098	1.082
	R_{CH3}	1.085	1.090	1.086		1.093	1.086
Pvdw (C$_1$)	R_{HCl}	1.277	1.280	1.281	1.298	1.298	1.276
	R_{HCl}	2.503	2.546	2.460	2.448	2.390	2.565
	R_{HC2}	2.503	2.566	2.416	2.414	2.503	2.621
	R_{CC}	1.291	1.290	1.283	1.301	1.313	1.321
	R_{CH1}	1.077	1.081	1.077	1.090	1.083	1.079
	R_{CH2}	1.087	1.092	1.087	1.099	1.095	1.088
	R_{CH3}	1.082	1.087	1.083	1.094	1.090	1.084
	α	86.6	78.3	87.1	87.3	82.1	81.6
TSvdw (C$_1$ or C$_s$)	R_{HCl}	1.278	1.281	1.281	1.297	1.300	1.278
	R_{HC}	2.253	2.276	2.255	2.236	2.263	2.253
	R_{CC}	1.287	1.287	1.280	1.297	1.312	1.287
	R_{CH1}	1.077	1.081	1.076	1.090	1.083	1.077
	R_{CH2}	1.082	1.087	1.083	1.094	1.090	1.082
	R_{CH3}	1.086	1.092	1.087	1.099	1.095	1.087
	α	22.9	0	33.3	31.6	67.6	22.9

[a] Values in parentheses and brackets correspond to QCISD(T)/6-31G(d,p) and QCISD(T)/cc-pVDZ results, respectively. [b] The geometries are depicted in Figures S1−S11 of Supporting Information. Bond distances are given in angstroms and angles are given in degrees.

Information contain the corresponding drawings. Tables 2−5 collect the energies relative to reactants (C$_2$H$_4$ and Cl) for all the structures collected in Table 1 (and depicted in Figures S1−S11 of Supporting Information). The corresponding absolute energies, the expectation values of the S^2 operator (providing information on the spin contamination), and the unprojected MP2 [6-31G(d,p), 6-311+G(d,p), 6-311++(3df,3pd), and aug-cc-pVDZ] absolute energies are included as Supporting Information (Tables S1−S8).

I. Geometries. Broadly speaking, according to Table 1, the geometrical parameters as computed with different methods and basis sets do not differ too much in the case of reactants (C$_2$H$_4$), products (CH$_2$ClCH$_2$•, CH$_3$ClCH•, C$_2$H$_3$•), transition structures for the 1,2-hydrogen shift (**TSm**), transition structures for the rotation around the C−C bond (**TSr**), and transition structures for abstraction (**TSabs**). Discrepancies of 0.08 Å for the C−Cl bond, 0.03 Å for the H(HCl)−C bond, 0.04 Å for the C−C bond, and 0.01 Å for the C−H bonds are detected. Inclusion of diffuse and polarization functions [6-311++G(3df,3pd)] leads, in general, to shorter C−C and C−Cl bond lengths while Dunning's aug-cc-pVDZ basis set usually renders larger bond lengths than Pople's 6-31G(d,p). Regarding methods, QCISD

Potential Energy Surface for Chlorine Atom

J. Phys. Chem. A, Vol. 104, No. 46, 2000 **10847**

TABLE 2: Energies (Relative to Reactants) in kcal/mol for Intermediates, Transition Structures, and Products of the Reaction between Ethylene and Chlorine Atom as Computed at Different Theoretical Levels Using the 6-31G(d,p) Basis Set[a]

system	MP2	Becke3LYP	QCISD[b]	QCISD(T)[c]	MP4SDTQ[c]	Becke3LYP[c]	QCISD(T)[d]	QCISD(T)/aug-cc-pVDZ[d]
Iadd	−5.6		−3.3	−4.1	−4.3	−13.2	−4.1	−7.0
TSadd	−6.3		−3.0	−3.5	−0.9	−13.5	−3.9	−7.5
TSabs	16.0 (−3.8)		18.4	18.3	22.3	9.3	17.2	11.2
Iabs	14.3		15.0	15.6	19.8	11.2	14.6	9.9
TSvdw	14.4	10.9	15.1	15.6	19.8	11.3	14.7	11.5
Pvdw	13.8	10.9	14.9	15.4	19.3	11.5	14.5	9.7
HCl C$_2$H$_3$•	} 17.1 (−3.9)	14.4 (−4.9)	17.6	18.3	22.7	14.9	17.4	13.1
CH$_3$ClCH•	−21.3 (1.2)	−23.1 (0.6)	−18.2	−18.2	−18.4	−23.0	−18.0	−19.1
TSm	28.3 (−1.6)	24.6 (−2.1)	34.2	33.2	33.3	25.1	33.0	28.5
CH$_2$ClCH$_2$•	−17.3 (1.1)	−19.5 (0.7)	−14.1	−14.1	−14.5	−18.9	−14.2	−16.6
TSr	−15.3 (0.2)	−16.4 (−0.2)	−12.1	−11.9	−12.4	−16.2	−12.0	−14.5
TSsb[e]	49.0 (0.1)	−13.2 (0.7)	52.6	52.3	55.2	42.7	50.4	44.8
Msb		40.6 (2.2)						

[a] The MP2 and Becke3LYP zero-point energies (relative to reactants and estimated by using the harmonic oscillator model) are given in parentheses (kcal/mol) for all the structures except those weakly bound. [b] No Hessian matrix was computed at the QCISD level of theory. [c] Single-point calculations on the MP2/6-31G(d,p) geometries. [d] Single-point calculations on the QCISD/6-31G(d,p) geometries. [e] The Becke3LYP TSsb is a $^2A_1$ while the rest of TSsb are $^2B_2$.

tends to provide longer C−C bonds than MP2 and DFT. However, DFT systematically predicts longer C−Cl bonds than MP2 and QCISD.

When considering structures involving long-distance interactions, the discrepancies are more notorious as can be seen in Table 1 (see structures **Iadd**, **TSadd**, **Iabs**, **Pvdw**, and **TSvdw**). Thus, for example, one of the C−Cl bond distances in the transition structure **TSadd** of the addition pathway (see Table 1) changes from 2.738 Å when computed with the 6-31G(d,p) basis set to 2.607 Å when the extended 6-311++G(3df,3dp) basis set is used at the MP2 level. Similar discrepancies are observed when employing different methodologies as shown in Table 1 for the C−Cl bond distances of **TSadd** computed with MP2 and QCISD methods. This is a direct consequence of the flatness of the PES in the regions of large intermolecular distances. However, predictions on the relative orientations of the two interacting species (see the values of different angles in Table 1 for **Iadd**, **TSadd**, **Iabs**, **Pvdw**, and **TSvdw**) are quite similar for all levels of theory employed, the only exception being the Becke3LYP/6-31G(d,p) method (see specially **TSvdw**). Furthermore, a number of structures (**Iadd**, **TSadd**, **Iabs**, **TSabs**) located at the MP2 and QCISD levels are not present on the DFT PES. The MP2/6-311+G(d,p) level also deserves further comments on this regard (see below).

II. Energies. The general trend (although with exceptions) observed for the relative energies of the structures located on the PES can be summarized as follows: (a) The (full optimized) QCISD structures tend to become less stable than those computed at the MP2 level while the opposite is true for the DFT structures (see Table 2). (b) For the series of Pople's basis sets, the structures become more stable as one uses more extended bases. Dunning's aug-cc-pVDZ basis set renders relative energies closer to Pople's extended basis sets results (see Tables 3−5). (c) Single-point QCISD(T) and MP4SDTQ calculations give, in general, less stable relative energies than MP2, whereas single-point DFT relative energies are usually more stable (see Tables 3−5).

QCISD(T)/6-31G(d,p)//MP2/6-31G(d,p) single-point calculations render relative energies similar to the QCISD/6-31G(d,p) ones. Also, Becke3LYP/6-31G(d,p)//MP2/6-31G(d,p) and Becke3LYP/6-31G(d,p) relative energies are rather similar. This confirms our previous observation (see previous section) that, in some cases, there are only small changes in geometries when using different methodologies. In the case of the structures involving two fragments (HCl and C$_2$H$_3$•; Cl and C$_2$H$_4$)

TABLE 3: Energies (Relative to Reactants) in kcal/mol for Intermediates, Transition Structures, and Products of the Reaction between Ethylene and Chlorine Atom as Computed at Different Theoretical Levels Using the 6-311+G(d,p) Basis Set

system	MP2	QCISD(T)[a]	MP4SDTQ[a]	Becke3LYP[a]
Iadd	−6.1	−4.8	−4.9	−11.9
TSadd	−6.6	−4.4	−1.8	−11.9
TSabs	12.9	14.8	18.6	8.5
Iabs				
TSvdw	11.4	12.2	16.2	9.8
Pvdw	11.0	12.1	15.9	10.2
HCl C$_2$H$_3$•	} 13.9	14.7	18.8	12.6
CH$_3$ClCH•	−22.0	−19.8	−19.7	−20.3
TSm	24.9	29.0	29.3	26.3
CH$_2$ClCH$_2$•	−18.4	−16.1	−16.2	−16.9
TSr	−16.4	−13.9	−14.1	−14.2
Msb	45.0	47.8	50.3	44.6

[a] Single-point calculations on the MP2/6-311+G(d,p) geometries.

TABLE 4: Energies (Relative to Reactants) in kcal/mol for Intermediates, Transition Structures, and Products of the Reaction between Ethylene and Chlorine Atom as Computed at Different Theoretical Levels Using the 6-311++G(3df,3pd) Basis Set

system	MP2[a]	QCISD(T)[b]	MP4SDTQ[b]	Becke3LYP[b]
Iadd	−9.8	−7.6	−8.0	−12.0
TSadd	−10.4	−7.5	−5.6	−12.1
TSabs	8.7	11.0	14.0	7.1
Iabs	8.1	9.1	12.4	7.9
TSvdw	8.2	9.3	12.6	8.4
Pvdw	7.8	9.1	12.3	8.5
HCl C$_2$H$_3$•	} 11.3	12.2	15.6	10.6
CH$_3$ClCH•	−25.7	−22.6	−22.9	−22.6
TSm	20.0	25.0	24.7	24.1
CH$_2$ClCH$_2$•	−21.8	−18.8	−19.1	−18.4
TSr	−20.0	−16.8	−17.3	−16.0
Msb	38.8	43.3	44.6	41.4

[a] No Hessian matrix was computed at the MP2 level of theory. [b] Single-point calculations on the MP2/6-311++G(3df,3pd) geometries.

interacting through long distance (van der Waals)[42] forces (see structures **Iadd**, **TSadd**, **Iabs**, **Pvdw**, and **TSvdw**) the above results suggest that the PES must be rather flat. Indeed, Table 1 shows that there is a remarkable reduction in the H(HCl)−C distance when passing from **Iabs** (2.232 Å) to **TSabs** (1.489 Å); however, the relative energies in Table 2 for both structures

TABLE 5: Energies (Relative to Reactants) in kcal/mol for Intermediates, Transition Structures, and Products of the Reaction between Ethylene and Chlorine Atom as Computed at Different Theoretical Levels Using the Aug-cc-pVDZ Basis Set

system	MP2	QCISD(T)[a]	MP4SDTQ[a]	Becke3LYP[a]
Iadd	−9.6	−7.7	−7.9	−12.6
TSadd	−10.0	−7.4	−5.3	−12.8
TSabs	10.2	12.5	16.2	7.1
Iabs	9.7	10.8	14.7	8.8
TSvdw	9.8	10.9	14.9	9.3
Pvdw	9.2	10.6	14.3	9.6
HCl C$_2$H$_3$•	} 13.0	14.0	18.0	11.8
CH$_3$ClCH•	−21.8	−19.0	−19.1	−21.4
TSm	24.0	28.7	28.7	24.3
CH$_2$ClCH$_2$•	−19.4	−16.6	−16.8	−18.4
TSr	−17.3	−14.4	−14.7	−15.7
Msb	43.9	46.9	49.7	41.7

[a] Single-point calculations on the MP2/aug-cc-pVDZ geometries.

are not too different, thus evidencing the flatness of the corresponding regions on the PES. On the other hand, the good agreement between the QCISD/6-31G(d,p) and the QCISD(T)/6-31G(d,p)//QCISD/6-31G(d,p) (see Table 2) seems to indicate that the considerable effort required to carry out QCISD(T) optimizations is barely justified for these systems.[43] Indeed, the QCISD(T)/6-31G(d,p) optimizations carried out for **Iadd** and **TSadd** rendered an energy barrier (see Table S1 of Supporting Information) and geometries (see Table 1) rather similar to those obtained at the QCISD/6-31G(d,p) level.

The highest level employed in the present calculations [QCISD(T)/aug-cc-pVDZ//QCISD/6-31G(d,p)] implies the use of quite sophisticated post-Hartree−Fock methodologies (coupled cluster theory)[44] and basis sets specially designed to be used in correlated calculations (Dunning's correlation consistent basis sets).[34] This level of theory seems to be appropriate to compute transition state geometries and energies for radical reactions.[45]

III. Bridged Structures. The unexpected preponderance of 1,2-dibromobutane in the product mixture from the radical bromination of 1-bromobutane[46] was attributed to a rate-enhancing effect of the bromo substituent on the vicinal position. Skell and co-workers interpreted this result by invoking a bridged radical.[24]

Two kinds of symmetrically bridged (C_{2v}) structures were located on the PES: (a) A $^2B_2$ structure was located at the MP2 and Becke3LYP levels of theory. The analysis of frequencies showed that while the MP2/6-31G(d,p) structure is a transition structure, the MP2/6-311+G(d,p), MP2/aug-cc-pVDZ and Becke3LYP/6-31G(d,p) structures are minima (see **TSsb** and **Msb** in Tables 1−5). (b) A $^2A_1$ structure with no imaginary frequencies (minimum) was located at all levels of theory (see **Iadd** in Tables 1−5) but for the Becke3LYP/6-31G(d,p) level. A transition structure ($^2A_1$) was located at this latter level (see **TSsb** in Tables 1 and 2).

IRC calculations[20] demonstrated that the **TSsb** structures (both $^2A_1$ and $^2B_2$) connect the two possible 2-chloroethyl radicals via a shuttle (or rocking)[28] motion (1,2 migration). The MP2/6-31G(d,p) transition structure **TSsb** ($^2B_2$) is too high (66.3 kcal/mol with respect to CH$_2$ClCH$_2$•), but the Becke3LYP/6-31G(d,p) barrier ($^2A_1$) is only 6.3 kcal/mol.

Our $^2A_1$ minimum structure (**Iadd**) corresponds to that previously reported by Guerra.[25] However, the very flat minimum structure ($^2B_2$) located by Guerra (MP2 calculations using double-ζ plus polarization and bond functions) at large C−Cl distances represents, according to our calculations [MP2/

6-31G(d,p)], a second-order saddle point (with two imaginary frequencies). Our $^2B_2$ minimum structure, located at different theoretical levels (see **Msb** in Tables 1−5), cannot be identified with the flat minimum reported by Guerra (while Guerra's $^2B_2$ minimum is about 0.3 kcal/mol stable to dissociation, our $^2B_2$ minimum is about 40−50 kcal/mol higher than the dissociation limit). In any case, our $^2B_2$ minimum structure is too high in energy as to play any significant role in the reaction mechanism.

On the other hand, we were unable to locate, at the MP2/6-31G(d,p) level, the bridged radical reported by Ihee et al. in their LMP2/LAV3P study.[28] It is a C_s structure and consequently differs from those (C_{2v}) reported by Guerra[25] and ours (see **Iadd** in Table 1). Moreover, the Becke3LYP/LAV3P minimum structure reported by Ihee et al.[28] coincides basically (both from the geometrical and energetic viewpoints) with our Becke3LYP/6-31G(d,p) structure **TSsb**.

IV. Rotation around the C−C Bond. The rotation around the C−C bond in 2-chloroethyl radical competes with the 1,2 migration motion mentioned in the previous section. Table 1 collects the most representative geometrical parameters of the transition structure associated with such a rotation as computed at different theoretical levels. The experimental barrier, obtained from ESR measurements, is 4.0 kcal/mol.[47] Engels et al.[23] computed (MRD-CI) a value (without optimization of the transition structure) of 4.3 kcal/mol while the MP4/6-311G-(d,p)//MP2/6-31G(d) barrier is 2.1 kcal/mol.[48] Ihee et al.[28] reported the values 1.8 (LMP2) and 3.5 (Becke3LYP) kcal/mol. Our higher theoretical level estimate for the rotational barrier [QCISD(T)/aug-cc-pVDZ//QCISD/6-31G(d,p)] is 2.1 kcal/mol (see Table 2). Furthermore, data in Tables 2−5 show that our computed barrier lies between 1.8 [MP2/6-311++G(3df,3pd)] and 3.1 kcal/mol [Becke3LYP/6-31G(d,p)], lower than the ESR estimated value and in good agreement with those of Ihee et al.[28]

V. 1,2 Hydrogen Shift. The most stable form of the chloroethyl radical is the 1-chloroethyl radical (see Tables 2−5). Table 1 collects the most representative geometrical parameters of the two radicals involved in the 1,2 hydrogen shift (CH$_3$-ClCH• and CH$_2$ClCH$_2$•) as well as the transition structure (**TSm**) connecting them as computed at different theoretical levels. The **TSm** transition structure has no symmetry (C_1) and the different theoretical levels employed provide rather similar geometrical parameters: C−H−C ≈ 69−70°, H−C$_1$ ≈ 1.300−1.315 Å, and H−C$_2$ ≈ 1.266−1.287 Å (see Table 1). The computed barrier height (relative to the 2-chloroethyl radical) does not exhibit a strong dependence on the method employed, oscillating between the 42−48 kcal/mol range (see Tables 2−5). The same conclusions apply to the geometries of the two radicals and their relative energies as can be seen from inspection of Tables 1−5.

According to Barat et al.[49] the barrier height for the interconversion between 1- and 2-chloroethyl radicals is 38 kcal/mol. This value was estimated as the sum of the relative stability of the two radicals (4 kcal/mol), ring strain (27 kcal/mol), and the barrier for abstraction of hydrogen by a carbon radical (7 kcal/mol). The agreement with our computed values for the barrier (42−48 kcal/mol) and the relative stability (2.3−4.1 kcal/mol) is rather good.

VI. Mechanistic Aspects. The geometrical and energetic information of the PES for the reaction between chlorine atom and ethylene presented in previous sections allows us to determine the mechanism through which such a reaction proceeds. The topology of the PES indicates the existence of two main pathways, namely, the addition and abstraction channels.

Potential Energy Surface for Chlorine Atom

J. Phys. Chem. A, Vol. 104, No. 46, 2000 **10849**
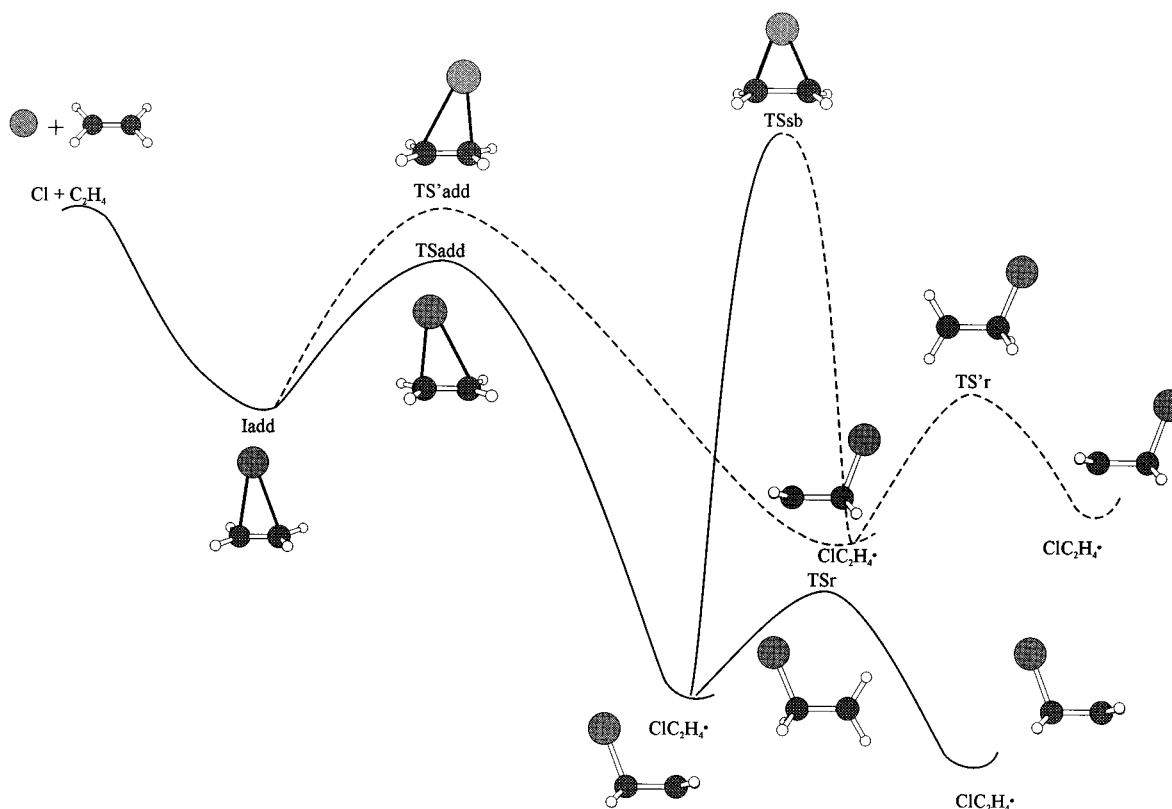
Figure 2. Addition channel for the reaction between ethylene and chlorine atom as computed at the MP2/6-31G(d,p) level of theory. The QCISD PES is similar to the one depicted in this figure (although the **TSsb** structure was not characterized because no Hessian matrix was computed at this level). MP2/aug-cc-pVDZ calculations provide a similar PES except for the **TSsb** structure that becomes a minimum and consequently does not connect the two equivalent CH$_2$ClCH$_2$• radicals anymore.
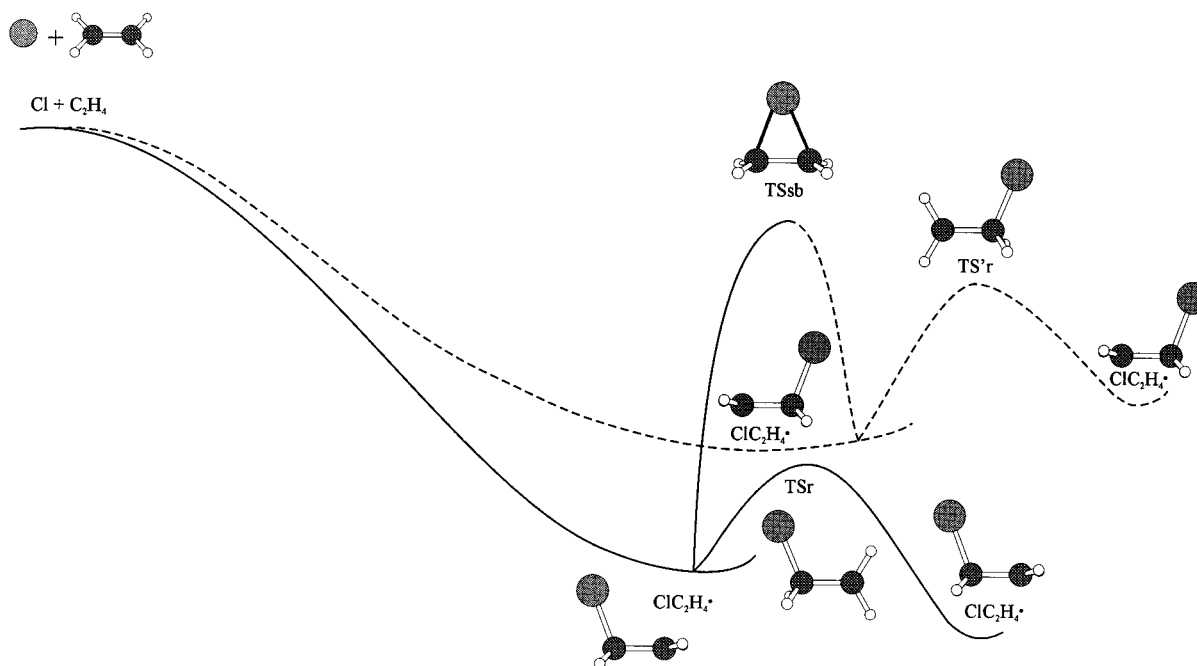
Figure 3. Addition channel for the reaction between ethylene and chlorine atom as computed at the Becke3LYP/6-31G(d,p) level of theory.

VIa. Addition Channel. Some preliminary results [MP2/6-31G(d,p) and QCI/6-31G(d,p) results in Table 2] have been reported elsewhere.[50] Therefore, only a brief comment on the mechanistic aspects emerging from Figure 2, emphasizing the new results obtained, is presented here.

Figure 2 shows a simplified qualitative scheme representing the addition channel arising from the MP2 and QCISD calcula-

tions [QCISD(T)/6-31G(d,p) and QCISD(T)/cc-pVDZ optimizations were also carried out for **Iadd** and **TSadd**; see below] and Figure 3 , the corresponding one from DFT (Becke3LYP) calculations.

According to the MP2 and QCISD calculations, as the ethylene and chlorine atom approach each other they form a stable molecular association with C_{2v} symmetry (symmetrically

Braña et al.

bridged structure; **Iadd**) which is connected through a C_s transition structure (asymmetrically bridged structure; **TSadd** or **TS′add**) with the 2-chloroethyl radical. It is important to remark at this point that the presence of **Iadd** is strictly needed from a topological point of view because **TSadd** is lower in energy than the reactants (see the negative value of the relative energy of this structure in Table 2). The fact that **TSadd** resulted lower in energy than **Iadd** at some levels of theory (for example, at the MP2 level; see Tables 2−5) is an artifact arising from spin contamination. Indeed, examination of the spin unprojected MP2 energies for **Iadd** and **TSadd** (see Table S8 of Supporting Information and ref 50) demonstrates that, as topologically required (optimizations are performed on the spin unprojected PES), **Iadd** is always lower in energy than **TSadd**.

The two possible equivalent conformations of the 2-chloroethyl radical are connected through a C_{2v} transition structure (**TSsb**; $^2B_2$ symmetrically bridged structure) located at the MP2/6-31G(d,p) level (an extensive search for a $^2A_1$ transition structure corresponding to a direct shuttle motion was unsuccessful). The energy barrier associated with this structure is too high in energy (49 kcal/mol) as to represent a plausible interconversion pathway (shuttle or rocking motion) connecting the two possible classical nonbridged 2-chloroethyl radicals. The same argument applies to the corresponding QCISD structure provided it were a transition structure (no Hessian matrix was computed at this level). The stereochemical control exercised by the chlorine atom reported in experimental studies on reactions involving haloethyl radicals[46] can be explained by the presence of the two bridged structures **Iadd** and **TSadd** located at both MP2 and QCISD levels on the addition pathway.[24] Consequently, the shuttle motion need not be invoked in the present mechanism unless one would consider that starting at the global minimum (CH$_2$ClCH$_2$•), going via **TSadd** to **Iadd** and then from **Iadd** back to CH$_2$ClCH$_2$• via **TS′add** (see Figure 2) is a kind of "indirect shuttle motion".[50] In any case, it represents an alternative to the direct shuttle motion associated with **TSsb**. Interestingly, the MP2/6-311+G(d,p) and MP2/aug-cc-pVDZ PESs do not contain any transition structure **TSsb** (as mentioned previously, the corresponding structures on these PESs were characterized as minima, **Msb**, when computing the Hessian matrix).

It must be pointed out that the barrier height (h) associated with **TSadd** ($h =$ **TSadd** − **Iadd**) is very small. Indeed, Table 2 shows that QCISD/6-31G(d,p) optimizations predict a barrier of only 0.3 kcal/mol that disappears when performing single-point QCISD(T)/aug-cc-pVDZ//QCISD/6-31G(d,p) calculations. Since we are dealing with rather small energy differences, we decided to perform QCISD(T) optimizations using 6-31G(d,p) and cc-pVDZ basis sets [no analytical gradients are implemented in the GAUSSIAN packages of programs[40,41] for the QCISD-(T) method, and to keep the problem tractable we performed the calculations using Dunning's basis sets without the augmented functions. According to our experience,[43] rather similar results should be expected from cc-pVXZ and aug-cc-pVXZ basis sets for ground states of neutral systems]. Both QCISD-(T)/6-31G(d,p) and QCISD(T)/cc-pVDZ predicted the existence of a barrier of 0.3 kcal/mol [the corresponding absolute energies can be found in the Supporting Information (Tables S1 and S4). See also Table 1 for the most representative geometrical parameters] in full agreement with the QCISD/6-31G(d,p) optimizations. The otherwise small discrepancies observed between the QCISD(T) optimizations and the single-point QCISD(T)//QCISD predictions become significant in this particular case where the barrier associated with **TSadd** is quite small.

Up to now, we considered the potential energy surface. It is well-known that, even though there is no general agreement,[51] it has been sometimes suggested that the activated state should be defined instead with reference to a free energy surface. In such a context, it can be argued, from a qualitative viewpoint, that the zero-point energy correction will tend to move **Iadd** above **TSadd** because this latter structure loses one vibrational mode with respect to **Iadd**. However, it should be also expected that the entropy contribution will act in the opposite direction (increasing the barrier) as **Iadd** is a much more loosely bound structure than **TSadd**. Unfortunately, **Iadd** is a weakly bound system (see its geometry in Table 1). Therefore, intermolecular vibrations are extremely anharmonic,[52] and the standard approach to compute the zero-point energy correction and the vibrational part of the entropy contribution, namely, the harmonic oscillator model, is not plausible. In any case, according to Singleton and Cvetanovic,[15] for a mechanism of the addition reaction like the one proposed here, with previous formation of a loosely bound complex without activation energy (**Iadd**) and its further conversion into products through a transition structure (**TSadd**) lower in energy than reactants, the global activation energy does not depend on the energy difference between **TSadd** and **Iadd**. It depends on the energy difference between **TSadd** and reactants (see eq VI and the discussion on negative activation energies in ref 15). The important point is the presence of structures **Iadd** and **TSadd,** and, as discussed above, our MP2, QCISD and QCISD(T) calculations support it (work in progress, involving calculations at the CASSCF and CASSCF MP2 levels, does provide additional support).

The two minima rotamers (anti conformations of the 2-chloroethyl radical) are connected through the transition structure **TSr** (or **TS′r**) which represents a relatively low energy barrier (1−4 kcal/mol; range of values based upon the theoretical and experimental estimates).

It is interesting to mention that there is a more stable form of the formed radical: the 1-chloroethyl radical (see Tables 2−5). However, the energy barrier (**TSm**) to pass from the 2-chloroethyl radical to the 1-chloroethyl radical is quite high [45.1 kcal/mol at the QCISD(T)/aug-cc-pVDZ//QCISD/6-31G-(d,p) level of theory]. Therefore, our calculations suggest that consideration of thermal decomposition of the more stable 1-chloroethyl radical in kinetic studies of the Cl + C$_2$H$_4$ reaction is not required, in agreement with predictions based upon qualitative assessments of the barrier height associated with **TSm**.[12,49]

The PES predicted by the DFT (Becke3LYP) method is somewhat different (see Figure 3): on one hand, no intermediate **Iadd** or transition structure **TSadd** are present. The chlorine atom approaches ethylene following a barrierless pathway leading to the 2-chloroethylene radical. On the other hand, the symmetrically bridged structure **TSsb** connecting the two equivalent conformations of classical nonbridged CH$_2$ClCH$_2$• belongs now to $^2A_1$ and is only 6.3 kcal/mol higher in energy than them [the corresponding $^2B_2$ transition structure located on the MP2/6-31G(d,p) PES becomes a minimum at the Becke3LYP/6-31G(d,p) level of theory according to a vibrational analysis].

In both cases (Figures 2 and 3), the addition reaction between chlorine atom and ethylene proceeds through a barrier-free mechanism with an exothermicity of −16.6 kcal/mol [−15.5 kcal/mol after adding the zero-point energy correction; ΔG (298

Potential Energy Surface for Chlorine Atom

J. Phys. Chem. A, Vol. 104, No. 46, 2000 **10851**
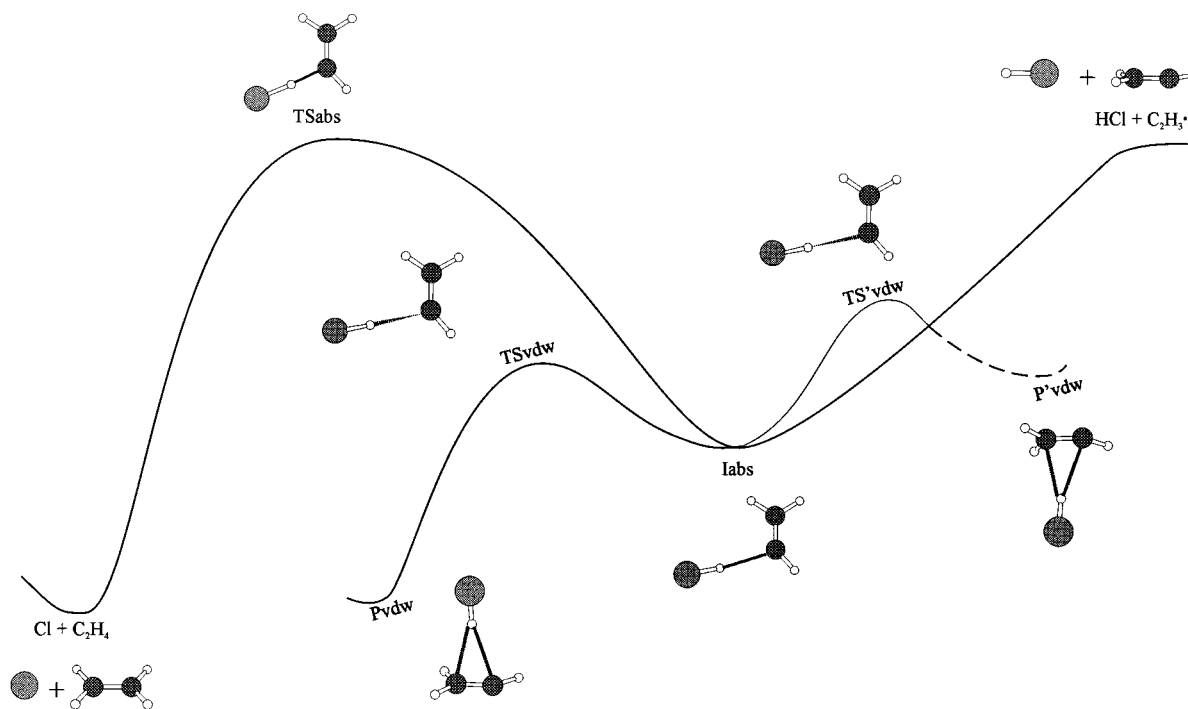
Figure 4. Abstraction channel for the reaction between ethylene and chlorine atom as computed at the MP2/6-31G(d,p), MP2/6-311++G(3df,3pd), MP2/aug-cc-pVDZ, and QCISD/6-31G(d,p) levels of theory.

K, 1 atm) = −9.4 kcal/mol] and −19.5 kcal/mol [−18.8 kcal/mol after adding the zero-point energy correction; ΔG (298 K, 1 atm) = −12.8 kcal/mol] as estimated at the QCISD(T)/aug-cc-pVDZ//QCISD/6-31G(d,p) and Becke3LYP/6-31G(d,p) levels, respectively (enthalpy and entropy contributions were obtained at the MP2/6-31G(d,p) and Becke3LYP/6-31G(d,p) levels, respectively), which is consistent with the experimental facts that the chlorine addition to ethylene occurs readily having little or no activation energy and with an exothermicity of −22 kcal/mol.[1] However, contrarily to the MP2 and QCISD predictions, the DFT calculations suggest a mechanism in which the direct shuttle motion could play a relevant role according to the model of Skell et al.[24] to explain the observed stereochemical control: a dynamic asymmetric bridging where the chlorine atom oscillates rapidly between the two carbon atoms (shuttle motion). Nevertheless, the barrier for the rotation around the C−C bond (3.1 kcal/mol), which is a competing mechanism, is much lower than the shuttling barrier (6.3 kcal/mol) both computed at the Becke3LYP/6-31G(d,p) level. Therefore, the mechanism emerging from the MP2, QCISD, and QCISD(T) calculations seems to be the most appropriate one to rationalize the experimental facts. It is an important, although somewhat frustrating, conclusion of the present study that the Density Functional Theory (Becke3LYP functional) leads to a rather different mechanism for the halogenation of alkenes than that suggested by the ab initio MP2, QCISD, and QCISD(T) methodologies.

VIb. Abstraction Channel. Figure 4 shows a simplified qualitative scheme representing the abstraction channel as computed at the MP2 [with 6-31G(d,p), 6-311++G(3df,3pd), and aug-cc-pVDZ basis sets] and QCISD/6-31G(d,p) levels of theory.

According to Figure 4, the abstraction reaction proceeds through a C_s transition structure **TSabs** to form a C_s intermediate **Iabs** in which the HCl molecule is almost formed and separated from the $C_2H_3\bullet$ final radical (see Table 1). The QCISD(T)/aug-cc-pVDZ//QCISD/6-31G(d,p) barrier height for this pathway

(h = **TSabs** − reactants) is 11.2 kcal/mol, which is consistent with an experimental activation energy of 3−7 kcal/mol.[9−12] Indeed, if we consider the zero-point energy correction [−3.8 kcal/mol at the MP2/6-31G(d,p) level of theory][53] as well as the 2RT term (∼2 kcal/mol at 500 K) we obtain an estimate for the activation energy of 9.4 kcal/mol. **Iabs** transforms into a C_1 bridged structure **Pvdw** through a C_1 transition structure **TSvdw** involving a rather low energetic barrier [less than 2 kcal/mol at the QCISD(T)/aug-cc-pVDZ//QCISD/6-31G(d,p) level]. The final products of the abstraction reaction (HCl and $C_2H_3\bullet$) obtained by the gradual separation of the HCl moiety in **Iabs** or **Pvdw** (for simplicity the connection between **Pvdw** and **P′vdw** with the products has not been traced out in Figure 4) are computed to be 13.1 kcal/mol endothermic at the QCISD(T)/aug-cc-pVDZ//QCISD/6-31G(d,p) level [9.2 kcal/mol after adding the zero-point energy correction; ΔG (500 K, 1 atm) = 4.8 kcal/mol, with the enthalpy and entropy contributions estimated at the MP2/6-31G(d,p) level],[53] which is not too far away from the value estimated from the thermodynamical data tables[1,8] (5−6 kcal/mol).

The MP2/6-311+G(d,p) abstraction pathway is slightly different (see Figure 5). Indeed, no minimum structure corresponding to the **Iabs** intermediate is present. IRC calculations show that **TSabs** is connected with **TSvdw** provided the C_s symmetry is forced. Otherwise, the reaction proceeds from the transition structure **TSabs** to the bridged structure **Pvdw** (the two equivalent structures **Pvdw** and **P′vdw** are connected through the transition structure **TSvdw**; see Figure 5). These results strongly suggest the presence of a branching point (see **BP** in Figure 5) in the reaction pathway; that is to say, "along the path one of the orthogonal motions that breaks the symmetry of the IRC changes its curvature from positive to negative then the IRC no longer leads to a minimum but to a saddle point of first order. The true reaction path does not preserve the symmetry and it must bifurcate from the IRC at the point (**BP** in Figure 5) where the curvature of the normal orthogonal mode changes its sign".[54]
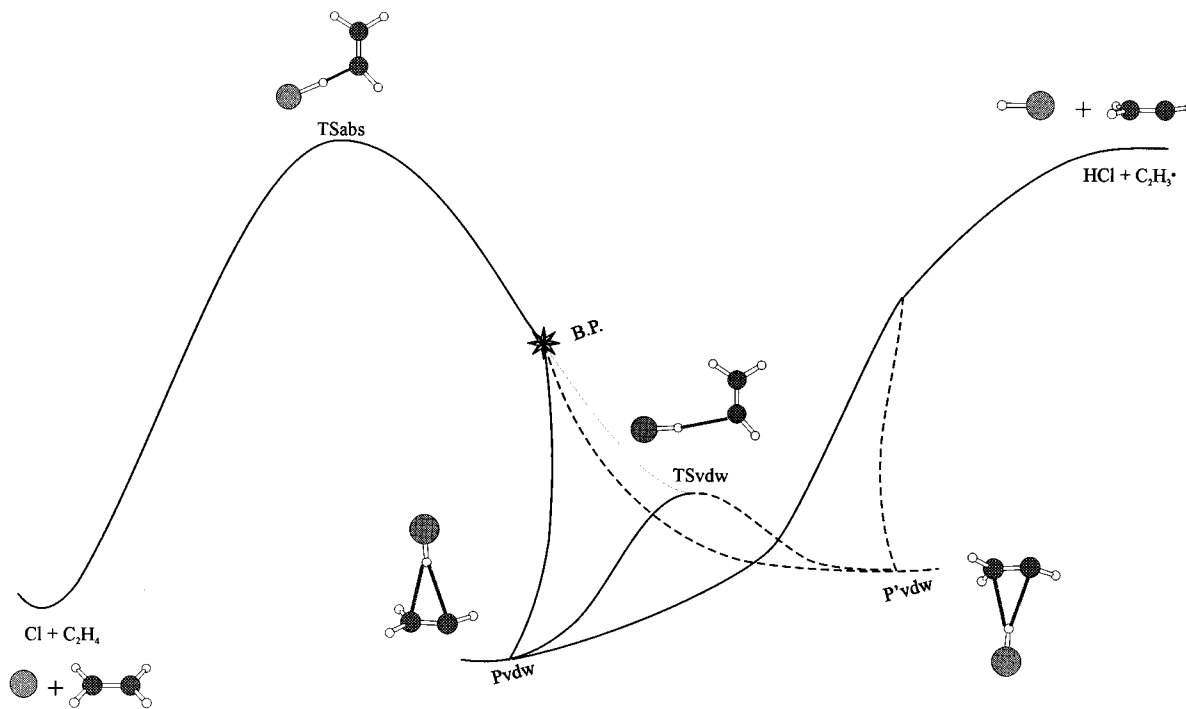
Figure 5. Abstraction channel for the reaction between ethylene and chlorine atom as computed at the MP2/6-311+G(d,p) level of theory.
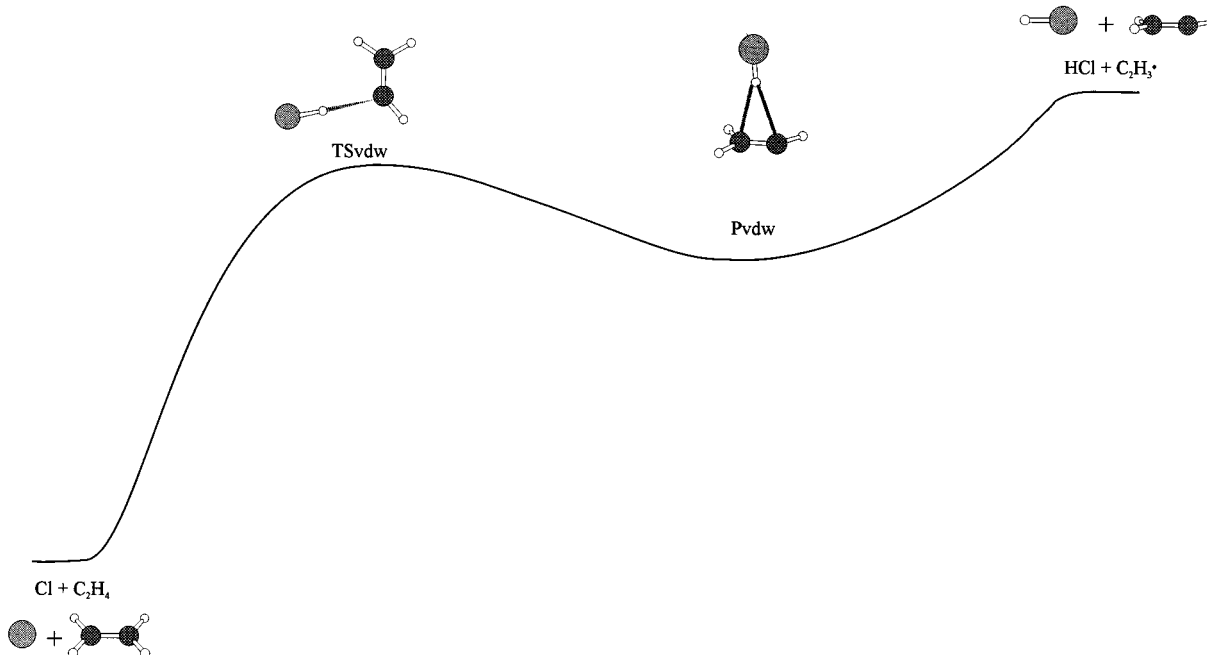
Figure 6. Abstraction channel for the reaction between ethylene and chlorine atom as computed at the Becke3LYP/6-31G(d,p) level of theory.

The Becke3LYP/6-31G(d,p) profile (see Figure 6) is quite different from the previous ones. Reactants transform into a C_1 bridged structure (**Pvdw**) through a C_1 transition structure (**TSvdw**). The C_s pathway involving **TSabs** and **Iabs** structures is not present on the DFT PES. The intermediate **Pvdw** leads to the final products (HCl, $C_2H_3\bullet$) following an endothermic pathway. It is important to remark that according to IRC/MP2 calculations while the transition structure connected with reactants in Figures 4 and 5 (**TSabs**) is a C_s structure, the IRC/Becke3LYP results indicate that the corresponding transition structure (**TSvdw**) has C_1 symmetry. Once again (see the previous section on the addition channel) DFT calculations lead to a PES that notably differs from those obtained with the rest of methods considered in the present work. The Becke3LYP/

6-31G(d,p) barrier associated with **TSvdw** in Figure 6 is 10.9 kcal/mol (due to the foreseeable anharmonicity of the intermolecular vibrations in structures such as **TSvdw**[52] no estimate of the zero-point energy correction was attempted), and the predicted endothermicity is 14.4 kcal/mol [9.5 kcal/mol after adding the zero-point energy correction; ΔG (500 K, 1 atm) = 6.4 kcal/mol, with the enthalpy and entropy contributions estimated at the Becke3LYP/6-31G(d,p) level].[53] These values are not far away from the corresponding QCISD(T)/aug-cc-pVDZ//QCISD/6-31G(d,p) values (9.4 and 9.2 kcal/mol, respectively). Therefore, in the case of the abstraction channel, although the PESs predicted by the several methodologies are quite different, all of them seem to be consistent with the

Potential Energy Surface for Chlorine Atom

J. Phys. Chem. A, Vol. 104, No. 46, 2000 **10853**

reported experimental activation barrier (3−7 kcal/mol)[9−12] and endothermicity (5−6 kcal/mol)[1,8] for this abstraction reaction.

Before finishing, we would like to stress the point that it is well-known that the presence of stable molecular complexes on the PES, as the ones described above, might significantly affect the reaction kinetics (i.e., activation energies and rate constants).[17,13a−c,g] Indeed, although the stabilization energies of such complexes were relatively small,[13h] the possibility of formation of new species with relatively weak bonds in radical recombination reactions needs to be investigated since they might play an important role in some particular processes where the entropic contributions are expected to be relatively small (for example, chemical processes taking place at polar stratospheric temperatures).[55]

Conclusions

Ab initio [MP2, QCISD, and QCISD(T)] and DFT (Becke3LYP) methods with different basis sets [6-31G(d,p), 6-311+G(d,p), 6-311++G(3df,3pd), and aug-cc-pVDZ] were used to explore the PES for the reaction between chlorine atom and ethylene. The main conclusions in the present study can be summarized as follows:

(a) Geometries: The geometrical parameters obtained with different methods and basis sets are rather similar but for the case of structures involving long distance interactions (van der Waals systems) in which, due to the flatness of the PES, quite large geometrical variations lead to relatively small energy changes.

(b) Energies: In general, the QCISD structures tend to become less stable than those computed at the MP2 level whereas the opposite is true for the DFT structures. The use of extended basis sets tends to provide greater stabilization energies and lower barrier heights. While single-point QCISD(T) and MP4SDTQ calculations render, in general, less stable relative energies than MP2, the single-point Becke3LYP relative energies are usually more stable. The QCISD(T)/aug-cc-pVDZ// QCISD/6-31G(d,p) barrier heights and relative energies are consistent with the experimental values for activation energies and exo/endothermicities, respectively.

(c) Addition channel: The MP2, QCISD, and QCISD(T) calculations show that the experimentally observed stereochemical control exercised by chlorine atom in reactions involving haloethyl radicals cannot be explained in terms of a direct shuttle motion where the chlorine atom oscillates rapidly between the two carbon atoms (blocking one side of the planar radical site). The existence of two bridged structures on the PES allows one to rationalize the experimental facts. The Becke3LYP PES suggests no stereochemical control as the barrier for the C−C rotation is lower than the barrier associated with the shuttle motion. These results complement the pioneering work by Engels and co-workers and some recent contributions on the subject. The presence of a minimum and a transition (both bridged) structure along the pathway connecting reactants and the product notably simplifies the interpretation of the dissociation mechanism making the assumption of Engels et al. that a given structure is at the same time a minimum and a transition structure unnecessary.

(d) Abstraction channel: A number of weakly bound (van der Waals) structures were located on the PES at the MP2 and QCISD levels. Under certain conditions, such as, for example, at polar stratospheric temperatures, such structures might play a relevant role in determining the mechanism through which the reaction between chlorine atom and ethylene proceeds. Slight modifications of the PES are observed when using the 6-311+G-

(d,p) basis set while the Becke3LYP PES is radically different. However, all the PESs seem to be consistent with the experimental data available on the activation barrier and endothermicity for this reaction.

As a general conclusion emerging from the present work, extreme care must be exercised to choose the appropriate theoretical level (method + basis set) to carry out calculations on reactions involving radicals. Different levels may provide unlike PES which in turn would suggest distinct mechanisms.

Supporting Information Available: Geometrical parameters for the following: the products of the addition reaction between ethylene and chlorine atom; **TSm** connecting $CH_2ClCH_2\cdot$ and $CH_3ClCH\cdot$ radicals; **Iadd**; **TSadd**; C_{2v}; **TSr**; the products of the abstraction reaction between ethylene and chlorine atom; **Iabs**; **TSabs**; **Pvdw**; and **TSvdw** (Figures S1−S11). Absolute energies for reactants, intermediates, transition structures, and products of the reaction between ethylene and chlorine atom as computed at different theoretical levels using the 6-31G(d,p) (Table S1), 6-311+G(d,p) (Table S2), 6-311++G(3df,3pd) (Table S3), and aug-cc-pVDZ basis set (Table S4). Values of $<S^2>$ before and after projection for the HF (Table S5), Becke3LYP (Table S6), and MP2 (Table S7) wavefunctions and MP2 unprojected absolute energies (Table S8) for the reactants, intermediates, transition structures, and products of the reaction between ethylene and chloride atom as computed with different basis sets. This material is available free of charge via the Internet at http://pubs.acs.org.

References and Notes

(1) Stevens, D. J.; Spicer, L. D. *J. Phys. Chem.* **1977**, *81*, 1217.
(2) Senkan, S. M. *Environ. Sci. Technol.* **1988**, *22*, 368.
(3) Tsang, W. *Combust. Sci. Technol.* **1990**, 74, 99.
(4) Rowland, F. S.; Molina, M. J. *Rev. Geophys. Space. Phys.* **1975**, 13, 1.
(5) Chameides, W. L.; Cicerone, R. J. J. *Geophys. Res.* **1978**, 83, 947.
(6) Cronn, D.; Robinson, E. *Geophys. Res. Lett.* **1979**, 6, 641.
(7) Singh, H. B.; Casting, J. F. *J. Atmos. Chem.* **1988**, 7, 261.
(8) Lee, F. S. C.; Rowland, F. S. *J. Phys. Chem.* **1977**, *81*, 1235.
(9) Parmar, S. S.; Benson, S. W. *J. Phys. Chem.* **1988**, *92*, 2652.
(10) Dobis, O.; Benson, S. W. *J. Am. Chem. Soc.* **1991**, *113*, 6377.
(11) Kaiser, E. W.; Wallington, T. J. *J. Phys. Chem.* **1996**, *100*, 4111.
(12) Pilgrim, J. S.; Taatjes, C. A. *J. Phys. Chem.* **1997**, *101*, 4172.
(13) See as representative examples: (a) Chen, Y.; Tschuikow-Roux, E.; Rauk, A. *J. Phys. Chem.* **1991**, *95*, 9832. (b) Chen, Y.; Rauk, A. J.; Tschuikow-Roux, E. *J. Phys. Chem.* **1991**, *95*, 9900. (c) Chen, Y.; Tschuikow-Roux, E. Phys. Chem. **1993**, 97, 3742. (d) Rayez, M.-T.; Rayez, J.-C.; Sawerysyn, J.-F *J. Phys. Chem.* **1994**, *98*, 11342. (e) Sekušak, S.; Liedl, K. R.; Sabljic, A. *J. Phys. Chem.* **1998**, *102*, 1583. (f) Farrell, J. T.; Taatjes, C. A. *J. Phys. Chem.* **1998**, *102*, 4846. (g) Jodkowski, J. T.; Rayez, M.-T.; Rayez, J.-C.; Bérces, T.; Dóbé, S. *J. Phys. Chem.* **1998**, *102*, 9219, 9230. (h) Alvarez-Idaboy, J. R.; Díaz-Acosta, I.; Vivier-Bunge, A. *J. Comput. Chem.* **1998**, 19, 811.
(14) Clementi, E., *MOTECC Modern Techniques in Computational Chemistry*; Escom: Leiden, 1991.
(15) Singleton, D. L.; Cvetanovic, R. J. *J. Am. Chem. Soc.* **1976**, *98*, 6812.
(16) Mozurkewich, M.; Benson, S. W. *J. Phys. Chem.* **1984**, *88*, 6429. (b) Mozurkewich, M.; Lamb, J. J.; Benson, S. W. *J. Phys. Chem.* **1984**, *88*, 6435. (c) Lamb, J. J.; Mozurkewich, M.; Benson, S. W. *J. Phys. Chem.* **1984**, *88*, 6441.
(17) Laidler, K. J., *Chemical Kinetics*, 3rd ed.; Harper & Row: New York, 1987.
(18) Suárez, D.; Sordo, J. A. *Chem. Commun.* **1998**, 385.
(19) Schlegel, H. B.; Sosa, C. *J. Phys. Chem.* **1984**, *88*, 1141.
(20) Gonzalez, C.; Schlegel, H. B. *J. Chem. Phys.* **1989**, 90, 2154. (b) Gonzalez, C.; Schlegel, H. B. *J. Phys. Chem.* **1990**, *94*, 5523.
(21) Rayón, V. M.; Sordo, J. A. *J. Phys. Chem.* **1997**, *101*, 7414.

(22) Hoz, T.; Sprecher, M.; Basch, H. *J. Phys. Chem.* **1985**, *89*, 1664.

(23) Engels, B.; Peyerimhoff, S. D.; Skell, P. S. *J. Phys. Chem.* **1990**, *94*, 1267.

(24) (a) Skell, P. S.; Tuleen, D. L.; Readio, P. D *J. Am. Chem. Soc.* **1963**, *85*, 2849, 2850. (b) Skell, P. S.; Traynham, J. G. *Acc. Chem. Res.* **1984**, *17*, 160.

(25) Guerra, M. *J. Am. Chem. Soc.* **1992**, *114*, 2077.

(26) Lloyd, R. V.; Wood, D. E. *J. Am. Chem. Soc.* **1975**, *97*, 5986.

(27) Knyazev, V. D.; Kalinovski, I.; Slagle, I. R. *J. Phys. Chem. A* **1999**, *103*, 3216.

(28) Ihee, H.; Zewail, A. H.; Goddard III, W. A. *J. Phys. Chem. A* **1999**, 103, 6638.

(29) Hay, P. J.; Wadt, W. R. *J. Chem. Phys.* **1985**, *82*, 284.

(30) Møller, C.; Plesset, M. S. *Phys. Rev.* **1934**, *46*, 618.

(31) Pople, J. A.; Head-Gordon, M.; Raghavachari, K. *J. Chem. Phys.* **1987**, *87*, 5968.

(32) Hohenberg, P.; Kohn, W. *Phys. Rev.* **1964**, *136*, B864. (b) Kohn, W.; Sham, L. J. *Phys. Rev.* **1965**, *140*, A1133.

(33) Hehre, W. J.; Radom, L.; Schleyer, P. v. R.; Pople, J. A. *Ab initio Molecular Orbital Theory*; Wiley: New York, 1986.

(34) Dunning, T. H., Jr. *J. Chem. Phys.* **1989**, *90*, 1007. (b) Kendall, R. A.; Dunning, T. H., Jr. *J. Chem. Phys.* **1992**, *96*, 6796. (c) Woon, D. E.; Dunning, T. H., Jr. *J. Chem. Phys.* **1993**, *98*, 1358.

(35) See for example: (a) Pudzianowski, A. T. *J. Chem. Phys.* **1995**, *102*, 8029. (b) Ford, T. A.; Steele, D. *J. Phys. Chem.* **1996**, *100*, 19336. (c) Süle, P.; Nagy, A. *J. Chem. Phys.* **1996**, *104*, 8524. (d) Liedl, K. R.; Sekušak, S.; Mayer, E. *J. Am. Chem. Soc.* **1997**, *119*, 3782. (e) Herrebout, W. A.; van der Veken, B. J *J. Am. Chem. Soc.* **1997**, *119*, 10446. (f) Liedl, K. R. *J. Chem. Phys.* **1998**, 108, 3199. (g) Everaert, G. P.; Herrebout, W. A.; van der Veken, B. J.; Lundell, J.; Räsäneu, M. *Chem. Eur. J.* **1998**, *4*, 321. (h) Samanta, U.; Chakrabarti, P.; Chandrasekhar, J. *J. Phys. Chem. A* **1998**, *102*, 8964.

(36) Boys, S. F.; Bernardi, F. *Mol. Phys.* **1970**, *19*, 553.

(37) Cook, D. B.; Sordo, J. A.; Sordo, T. L. *Int. J. Quantum Chem.* **1993**, *48*, 375.

(38) Simon, S.; Duran, M.; Dannenberg, J. J. *J. Phys. Chem.* **1999**, *103*, 1640.

(39) Sordo, J. A. *J. Chem. Phys.* **1997**, *106*, 6204. (b) Rayón, V. M.; Sordo, J. A. *J. Chem. Phys.* **1997**, *107*, 7912. (c) Rayón, V. M.; Sordo, J. A. *Theor. Chem. Acc.* **1998**, *99*, 68. (d) Rayón, V. M.; Sordo, J. A. *J. Chem. Phys.* **1999**, *110*, 377. (e) López, J. C.; Alonso, J. L.; Lorenzo, F. J.; Rayón, V. M.; Sordo, J. A. *J. Chem. Phys.* **1999**, *111*, 6363.

(40) *Gaussian 94*, Revision E.1, Frisch, M. J.; Trucks, G. W.; Schlegel, H. B.; Gill, P. M. W.; Johnson, B. G.; Robb, M. A.; Cheeseman, J. R.; Keith, T.; Petersson, G. A.; Montgomery, J. A.; Raghavachari, K.; Al-Laham, M. A.; Zakrzewski, V. G.,; Ortiz, J. V.; Foresman, J. B.; Cioslowski, J.; Stefanov, B. B.; Nanayakkara, A.; Challacombe, M.; Peng, C. Y.; Ayala, P. Y.; Chen, W.,; Wong, M. W.; Andres, J. L.; Replogle, E. S.,; Gomperts, R.; Martin, R. L.; Fox, D. J.; Binkley, J. S.; Defrees, D. J.; Baker, J.; Stewart, J. P.; Head-Gordon, M.; Gonzalez, C.; and Pople, J. A.; Gaussian, Inc., Pittsburgh, PA, 1995.

(41) *Gaussian 98*, Revision A.6, Frisch, M. J.; Trucks, G. W.; Schlegel, H. B.; Scuseria, G. E.; Robb, M. A.; Cheeseman, J. R.; Zakrzewski, V. G.; Montgomery, J. A., Jr.; Stratmann, R. E.; Burant, J. C.; Dapprich, S.; Millam, J. M.; Daniels, A. D.; Kudin, K. N.; Strain, M. C.; Farkas, O.; Tomasi, J.; Barone, V.; Cossi, M.; Cammi, R.; Mennucci, B.; Pomelli, C.; Adamo, C.; Clifford, S.; Ochterski, J.; Petersson, G. A.; Ayala, P. Y.; Cui, Q.; Morokuma, K.; Malick, D. K.; Rabuck, A. D.; Raghavachari, K.; Foresman, J. B.; Cioslowski, J.; Ortiz, J. V.; Stefanov, B. B.; Liu, G.; Liashenko, A.; Piskorz, P.; Komaromi, I.; Gomperts, R.; Martin, R. L.; Fox, D. J.; Keith, T.; Al-Laham, M. A.; Peng, C. Y.; Nanayakkara, A.; Gonzalez, C.; Challacombe, M.; Gill, P. M. W.; Johnson, B.; Chen, W.; Wong, M. W.; Andres J. L.; Gonzalez, C.; Head-Gordon, M.; Replogle, E. S.; and Pople, J. A.; Gaussian, Inc., Pittsburgh, PA, 1998.

(42) Hobza, P.; Zahradník, R. *Intermolecular Complexes. The Role of van der Waals Systems in Physical Chemistry and in Biodisciplines*; Academia, Prague, 1988.

(43) Feller, D.; Sordo, J. A. *J. Chem. Phys.* **2000**, *112*, 5604.

(44) Bartlett, R. J.; Stanton, J. F. in *Reviews in Computational Chemistry V*; Lipkowitz, K. B.; Boyd, D. B., Eds; VCH: New York, 1994.

(45) Chuang, Y.-Y.; Coitiño, E. L.; Truhlar, D. G. *J. Phys. Chem. A* **2000**, *104*, 446.

(46) Thaler, W. *J. Am. Chem. Soc.* **1963**, *85*, 2607.

(47) Chen, K. S.; Elson, I. H.; Kochi, J. K. *J. Am. Chem. Soc.* **1973**, *95*, 5341.

(48) Chen, Y.; Tschuikow-Roux, E. *J. Phys. Chem.* **1992**, *96*, 7266.

(49) Barat, R. B.; Bozzelli, J. W. *J. Phys. Chem.* **1992**, *96*, 2494.

(50) Braña, P.; Menéndez, B.; Fernández, T.; Sordo, J. A. *Chem. Phys. Lett.* **2000**, *325*, 693.

(51) Laidler, K. J, *Theories of Chemical Reaction Rates*; McGraw-Hill: New York, 1969; pp 76−79 and references therein.

(52) Sun, S.; Berstein, E. R. *J. Phys. Chem.* **1996**, *100*, 13348.

(53) It must be stressed that neither **TSabs** (see its geometry in Table 1) nor the abstraction products (HCl, C$_2$H$_3$•) are weakly bound associations, and therefore the harmonic approximation can be applied.

(54) Bosch, E.; Moreno, M.; Lluch, J. M.; Bertrán, J. *Chem. Phys. Lett.* **1985**, 160, 543. (b) Quapp, W.; Hirsch, M.; Heidrich, D. *Theor. Chem. Acc.* **1998**, 100, 285. (c) Valdés, H.; Rayón, V. M.; Sordo, J. A. *Chem. Phys. Lett.* **1999**, 309, 265.

(55) Molina, M. J.; Molina, L. T.; Golden, D. M. *J. Phys. Chem.* **1996**, *100*, 12888.